# SULFUR-BASED LITHIUM-ORGANIC ELECTROLYTE SECONDARY BATTERIES

Gerhard L. Holleck, et al

EIC, Incorporated

Prepared for:

Army Electronic Command

November 1975

Research and Development Technical Report

ECOM - 74-0072-6



# SULFUR-BASED LITHIUM-ORGANIC ELECTROLYTE SECONDARY BATTERIES

G. L. Holleck
J. R. Driscoll

EIC, Incorporated
55 Chapel Street
Newton, MA 02158

NOVEMBER 1975
Sixth Quarterly Report for Period 4 March 1975 - 3 June 1975

DISTRIBUTION STATEMENT

Approved for Public Release;
Distribution Unlimited



Prepared for
ECOM

US ARMY ELECTRONICS COMMAND FORT MONMOUTH, NEW JERSEY 07703

## NOTICES

### Disclaimers

The findings of this report are not to be construed as an official Department of the Army position, unless so designated by other authorized documents.

The citation of trade names and names of manufacturers in this report is not to be construed as official government endorsement or approval of commercial products or services referenced herein.

### Disposition

Destroy this report when it is no longer needed. Do not return to the originator.

UNCLASSIFIED

SECURITY CLASSIFICATION OF THIS PAGE (When Data Entered)

| REPORT DOCUMENTATION PAGE | | READ INSTRUCTIONS BEFORE COMPLETING FORM |
|---|---|---|
| 1. REPORT NUMBER<br>ECOM-74-0072-6 | 2. GOVT ACCESSION NO. | 3. RECIPIENT'S CATALOG NUMBER |
| 4. TITLE (and Subtitle)<br>SULFUR-BASED LITHIUM-ORGANIC ELECTROLYTE SECONDARY BATTERIES | | 5. TYPE OF REPORT & PERIOD COVERED<br>Sixth Quarterly Report<br>4 Mar 1975 - 3 Jun 1975<br>6. PERFORMING ORG. REPORT NUMBER<br>C-405 |
| 7. AUTHOR(s)<br>Gerhard L. Holleck and Joseph R. Driscoll | | 8. CONTRACT OR GRANT NUMBER(s)<br>DAAB07-74-C-0072 |
| 9. PERFORMING ORGANIZATION NAME AND ADDRESS<br>EIC, Inc.<br>55 Chapel Street, Newton, Ma. 02158 | | 10. PROGRAM ELEMENT, PROJECT, TASK AREA & WORK UNIT NUMBERS<br>1T1 61102 A34A 02452 |
| 11. CONTROLLING OFFICE NAME AND ADDRESS<br>U.S. Army Electronics Command<br>Attn: AMSEL-TL-PR<br>Fort Monmouth, N.J. 07703 | | 12. REPORT DATE<br>NOVEMBER 1975<br>13. NUMBER OF PAGES<br~~34~~ 42 |
| 14. MONITORING AGENCY NAME & ADDRESS(if different from Controlling Office) | | 15. SECURITY CLASS. (of this report)<br>UNCLASSIFIED<br>15a. DECLASSIFICATION/DOWNGRADING SCHEDULE |

16. DISTRIBUTION STATEMENT (of this Report)

Approved for Public Release; distribution unlimited.

17. DISTRIBUTION STATEMENT (of the abstract entered in Block 20, if different from Report)

18. SUPPLEMENTARY NOTES

19. KEY WORDS (Continue on reverse side if necessary and identify by block number)

Organic Solvents, Titanium Sulfide Electrodes, Lithium Anodes, Intercalation Compounds, Titanium-Vanadium Sulfide Electrodes.

20. ABSTRACT (Continue on reverse side if necessary and identify by block number)

This program is aimed at developing a rechargeable organic-electrolyte lithium battery to operate over the range -40 to +160°F, have an energy density approaching 100 Whr/lb, a cycle life in excess of 500, and high charge retention. The approach is to use positive electrodes based on higher sulfides of Nb, Ti and V.

DD FORM 1 JAN 73 1473 EDITION OF 1 NOV 65 IS OBSOLETE S/N UNCLASSIFIED

SECURITY CLASSIFICATION OF THIS PAGE (When Data Entered)

20. Abstract (Cont.)

Ti disulfides and trisulfides were prepared thermally. Both sulfides are electrochemically active and show similar overall behavio.. Charge-discharge cycles in PC and methyl acetate ($LiAlCl_4$, $LiClO_4$) electrolytes are characterized by relatively flat voltage plateaus with mid-discharge potentials of 2.0V.

The capacity is especially large during the first discharge of $TiS_3$. Upon extended cycling (~100 cycles), $TiS_3$ and $TiS_2$ operated at constant capacity of approximately 0.6 equivalent per mol of sulfide. The discharge cutoff potential, the sulfide preparation, and the solvent appear to affect the cycling behavior.

Charge and discharge reactions of $TiS_2$ electrodes are relatively rapid. Typical electrodes deliver 60% of their capacity at current densities above 3 $mA/cm^2$. Diffusion of $Li^+$ ions in the sulfide and the electrolyte appear to be rate limiting.

Titanium-vanadium alloy trisulfide electrodes show lower discharge potentials (1.7V). Capacity and cycling behavior are similar to $TiS_3$.

TABLE OF CONTENTS

## LIST OF FIGURES

LIST OF FIGURES
(Continued)

## LIST OF TABLES

# I. INTRODUCTION

The overall aim of this program is to develop a rechargeable lithium battery utilizing an organic solvent. Specifications are operation over the range -40 to +160°F (-40 to +70°C), energy density approaching 100 Whr/lb, a cycle-life in excess of 500, and high charge retention. A system meeting all these specifications would represent a considerable advance in the state of the art.

An analysis of possible alternatives suggests the likelihood of developing such batteries with positive electrodes based on sulfur. Two general classes are promising: soluble sulfur positives, and positives based on higher sulfides of transition metals, particularly on sulfur-rich compounds of titanium, niobium and vanadium. Initial work was carried out in both areas.

After the second quarter, since only one of the two approaches towards sulfur based cathodes could be continued, we decided to concentrate on the transition metal sulfides as they offer more immediate prospects for practical use.

Transition metal disulfides and trisulfides, especially those of Nb and Ti, were prepared thermally. Initial attempts of electrochemical formation of higher sulfides of niobium proved unsuccessful. The thermally synthesized aulfides were characterized by scanning electron microscopy and by x-ray diffraction. All sulfides were electrochemically active and exhibited similar overall behavior. Charge-discharge cycles in PC/$LiAlCl_4$ electrolytes showed good reversibility and flat voltage plateaus with mid-discharge potentials of ~2.0V. In half-cell tests, and in tests with an experimental battery configuration, the capacity during the first discharge cycle was always significantly larger than for the second cycle, but there was little change thereafter. The system had a fairly high rate capability (C rate) with only moderate penalities in potential and capacity. Capacity and discharge potential, especially at higher rates, improved at higher temperatures. Capacity losses observed during galvanostatic cycling would be restored in part by potentiostatic charging.

Scanning electron micrographs showed that $NbS_2$ layers swell and crack during discharge. Good results with bonded powder electrodes demonstrated that the use of thin film configurations is not necessary and, for practical batteries, probably not even desirable. The effect

of the nature and concentration of the electrolyte led to a better understanding of the mechanism of transition metal sulfide electrodes: The layer structure of the sulfide is retained during discharge, which involves a valency change of the metal atom. To compensate for the remaining negative charge (no $S^{2-}$ leaves the lattice), cations are intercalated into the octahedral interstices between the two sulfur-sulfur layers.

Attempts to further increase the capacity by also intercalating additional non-metals (sulfur, iodine) were not successful. It appears that either they cannot be intercalated or they are electrochemically inactive. Electrochemical characterization and study of the cycle behavior was expanded, especially for titanium sulfides. While the first discharge of $NbS_3$ occurs at a lower voltage than the disulfide, this difference was not observed with $TiS_3$. Material utilization during later cycles appeared to be better for $NbS_3$ than for $TiS_3$.

The product of the first discharge cycle is only partially rechargeable for all sulfides. For $NbS_2$, $NbS_3$ and $TiS_2$, the non-rechargeable part of the first cycle capacity is primarily associated with the initial part of the first discharge. In contrast, $TiS_3$ shows high reversibility during the initial part of the first discharge; however, the later part of the first discharge is not rechargeable.

The overall structure of the sulfides influences reversibility strongly during continued cycling. Structure depends on preparation procedures. $NbS_3$ prepared by a two-step procedure showed e/S values of 0.46 after 48 full charge-discharge cycles.

Initial efficiencies of up to 1.0 and 0.6 electrons per S were observed for trisulfides and disulfides respectively. After approximately 10 to 30 cycles, utilization of about 0.3 to 0.5 e/S were measured. Since our main interest was to study as many facets as possible, no optimization was performed, and also the cycle data cannot be considered as life tests. In practical terms, an e/S ratio of 0.8 translates into an active material energy density (actual mid-discharge voltage) of 240 Whr/lb for Nb sulfides and over 300 Whr/lb for Ti sulfides. e/S values of 0.3 for $TiS_3$ still show energy densities (based on the active material and practical voltages) of 143 Whr/lb. Vanadium sulfides prepared under identical conditions proved to date electrochemically practically inactive. Molybdenum disulfide is also electrochemically active. Discharge voltages are between 1.15 and 1.55V.

The initial work was carried out mainly with niobium sulfides. During the present reporting period the characterization and electrochemical behavior of titanium and titanium alloy sulfides was investigated more closely. Titanium sulfides are of special interest for practical applications due to the ready availability and the relatively low equivalent weight of titanium.

## II. EXPERIMENTAL WORK AND DISCUSSION

### A. Cycle Testing of Titanium Sulfide Electrodes

#### 1. Performance During Extended Charge-Discharge Cycling

##### (a) Titanium Disulfide

Experimental: The $TiS_2$ foil was prepared as previously described (1) by reaction of a titanium metal flag with sulfur vapor at 750°C in an evacuated quartz tube. The test cell was a simulated battery configuration with the $TiS_2$ foil in a tight package with a surrounding lithium foil and a glass fiber separator. A lithium reference electrode was used. The active electrode area was 6.6 $cm^2$ with $1.02 \times 10^{-3}$ mol $TiS_2$.

The $TiS_2$ was cycled between the potentials of +1.5 and +2.8V vs. Li at 5.2 mA (0.78 $mA/cm^2$). The electrolyte was 1M $LiClO_4$ in propylene carbonate (PC), prepared from freshly distilled PC and dried three times with 5A molecular sieve after the $LiClO_4$ dissolution.

The cell was cycled continuously until it failed at approximately the 120th cycle when the glass vial container fractured with attendant loss of electrolyte. The $TiS_2$ foil and surrounding glass fiber separator were recovered, the exterior surfaces of the fiber were cleaned of most of the accumulated lithium residue, and the package reassembled into a new cell with a fresh lithium counter electrode and reference. Cycling was then continued. The glass cell fractured due to pressure from the accumulation of a lithium residue between the lithium counter electrode and the glass separator. The residue was a compacted gray powder. It appeared to be primarily Li metal. Small samples reacted vigorously with water. No further characterizations were attempted at this time.

Results: The first discharge showed a capacity of 0.757 equivalent per mol $TiS_2$. On the subsequent recharge, the electrode accepted 0.612 equiv/mol $TiS_2$. For the next 50 discharges the average yield was 0.612 equiv/mol $TiS_2$ with extremes of 0.600 and 0.627. The yield for the first 51 recharges averaged 0.612 equiv/mol $TiS_2$ with extremes of 0.600 and 0.627. These numbers indicate good capacity reversibility during the first 51 cycles. After 51 cycles the capacity decreased but reversibility continued to be good. Table 1 lists the discharge and charge yields for the first, the fifth and every subsequent fifth cycle. The poor capacity reversibility recorded on the 120th cycle was probably caused by the cracking of the cell. The cell cycled 24 more times after cycle 120. These cycles were shorter and very erratic in potential.

Table 1

Capacity of a $TiS_2$ Foil Cycled Galvanostatically Between +1.5V and +2.8V vs. Li

| Capacity (equiv/mol $TiS_2$) | | | Capacity (equiv/mol $TiS_2$) | | |
|---|---|---|---|---|---|
| Cycle No. | Discharge | Charge | Cycle No. | Discharge | Charge |
| 1 | $0.75_7$ | $0.61_2$ | 65 | $0.57_8$ | $0.58_0$ |
| 5 | $0.61_0$ | $0.60_8$ | 70 | 0.576 | 0.580 |
| 10 | $0.60_8$ | $0.61_0$ | 75 | $0.58_6$ | $0.58_6$ |
| 15 | $0.60_1$ | $0.60_6$ | 80 | $0.56_3$ | $0.56_5$ |
| 20 | $0.61_2$ | $0.62_5$ | 85 | $0.57_2$ | $0.57_4$ |
| 25 | $0.60_8$ | $0.60_8$ | 90 | $0.55_7$ | 0.557 |
| 30 | $0.61_0$ | $0.61_8$ | 95 | $0.55_7$ | $0.55_5$ |
| 35 | $0.61_8$ | $0.62_1$ | 100 | $0.54_0$ | $0.54_2$ |
| 40 | $0.62_3$ | $0.62_5$ | 105 | $0.53_3$ | 0.537 |
| 45 | $0.61_4$ | $0.61_2$ | 110 | $0.53_3$ | $0.52_7$ |
| 50 | $0.62_0$ | $0.61_6$ | 115 | $0.51_4$ | $0.50_3$ |
| 55 | $0.59_7$ | $0.59_5$ | 120 | $0.46_5$ | $0.43_1$ |
| 60 | $0.58_8$ | $0.58_9$ | | | |

The reasons for the loss of capacity after the 50th cycle are not clear. There is no indication that changes are occurring in the potential during discharge or recharge until the 80th cycle. Figures 1-3 show the potential vs. time for this cell during discharge and recharge for the 10th, 50th, and 110th cycles. On the 10th cycle (Fig. 1), the mid-discharge potential (MDP) was 2.14V and the mid-recharge potential (MRP) was 2.18V. Both the discharge and recharge show a single plateau and the inflections at the end of each are sharp. On the 50th cycle (Fig. 2), the potential vs. time is quite similar to the 10th cycle with a MDP of 2.16V and a MRP of 2.22V. Here again the inflections at the end of discharge and recharge are sharp, and both discharge and recharge are a single plateau. The 110th cycle potential vs. time curve (Fig. 3) illustrates changes that first became evident on the 80th cycle. The discharge still has a single plateau, but shortly after the halfway point the potential exhibits an increased negative slope and decays gradually to the +1.5V lower limit. There is no sharp inflection at the end of the discharge. The recharge potential curve now shows two plateaus: a short one at ∿+1.65V which first became evident on the 95th cycle as a small inflection on the curve and which increased steadily in length, and a longer one similar to those seen in Figs. 1 and 2. The initial portion has a slightly greater slope. The shape of this curve after the halfway point is quite similar to that of the 10th and 50th cycles.

After the cell failure, the $TiS_2$ electrode package was reassembled with a new Li electrode and electrolyte and cycling continued under the same conditions (between +1.5 and +2.8V at 5.2 mA). The capacity increased slowly with cycling and stabilized at $\sim 0.39_5$ both on discharge and recharge. At the end of this reporting period the electrode reached 40 cycles after reassembly. Table 2 contains the yield data for the first and fifth cycle and every subsequent fifth cycle. The capacity reversibility is good for this electrode. The increase in capacity is accompanied by an increase in potential reversibility. Figures 4 and 5 show the potentials for the 5th and the 25th cycles. The 5th cycle MDP was 1.98V and the MRP was 2.25V. For the 25th cycle, the MDP was 2.08V and the MRP was 2.14V. The shape of the curves also improves with cycling. On the 25th cycle the end of both the discharge and charge curves are marked by sharp inflections, while in the 5th cycle the curves change more gradually.

In summary, we find extremely good reversibility during cycling of $TiS_2$. After the second cycle no changes in capacity or shape of the current potential curve were observed for the next 50 cycles. These cycles consisted of full charge-discharge cycles at the rather high C/3 rate. Further cycling was characterized by a slow continuous capacity decrease and a sloping potential towards the end of discharge. Whether this is an intrinsic property of the cycled titanium sulfide or caused indirectly by the change in the lithium electrode has not been established. After 100 cycles the capacity was still nearly 90% of the second cycle capacity. Cell failure was due to mechanical effects (expansion) of the lithium electrode.

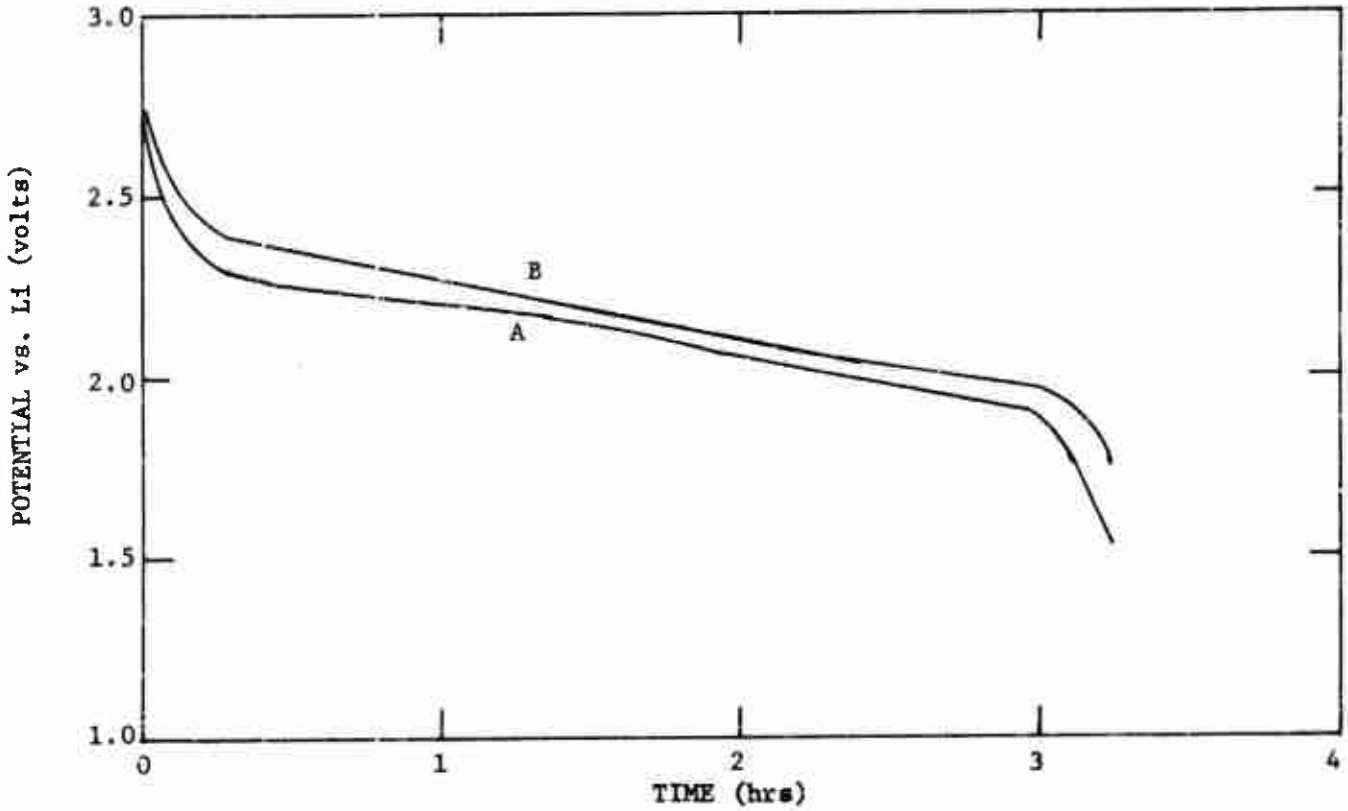


Fig. 1: Tenth discharge (A)-recharge (B) cycle for $TiS_2$. PC, 1M $LiClO_4$, i = 0.78 $mA/cm^2$.

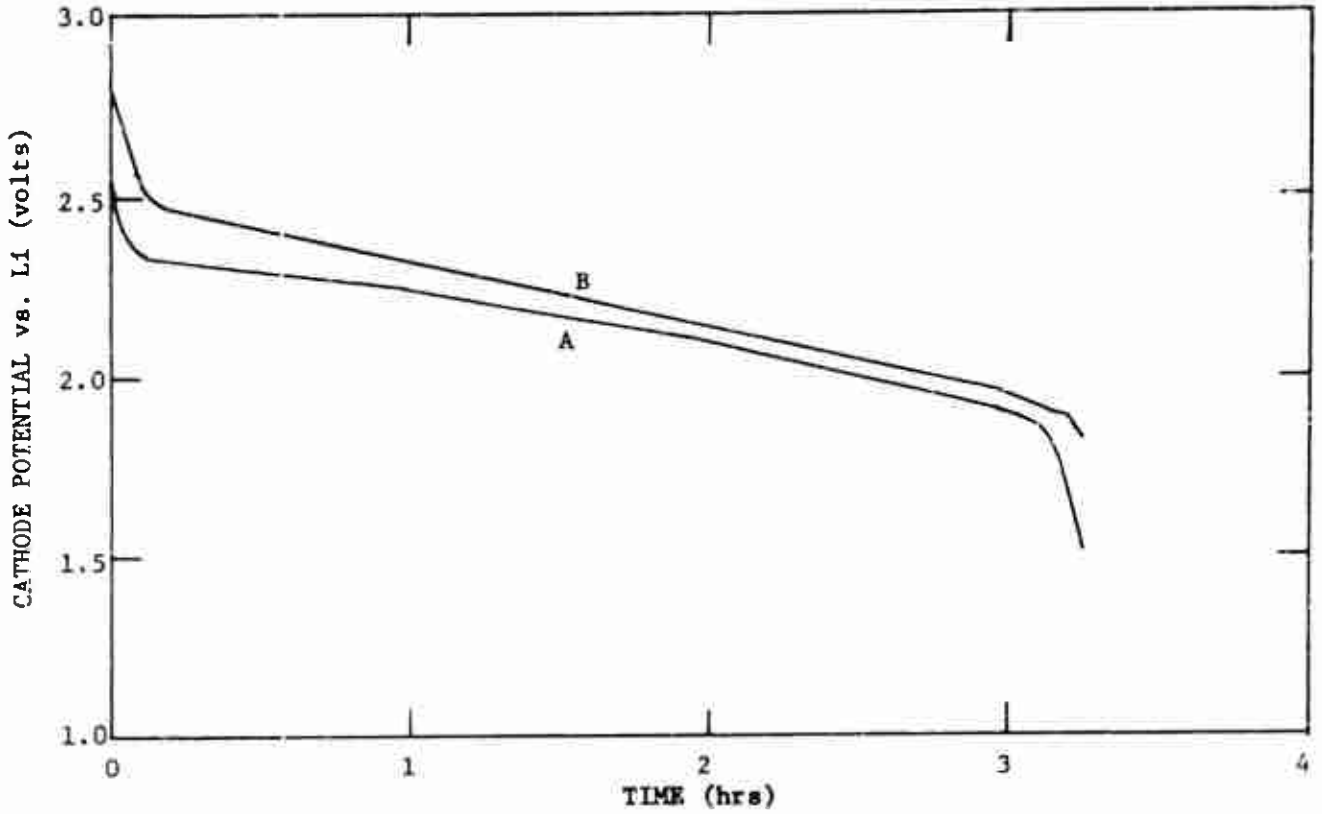


Fig. 2: Fiftieth discharge (A)-charge (B) cycle of $TiS_2$. PC, 1M $LiClO_4$, i = 0.78 mA/cm$^2$.

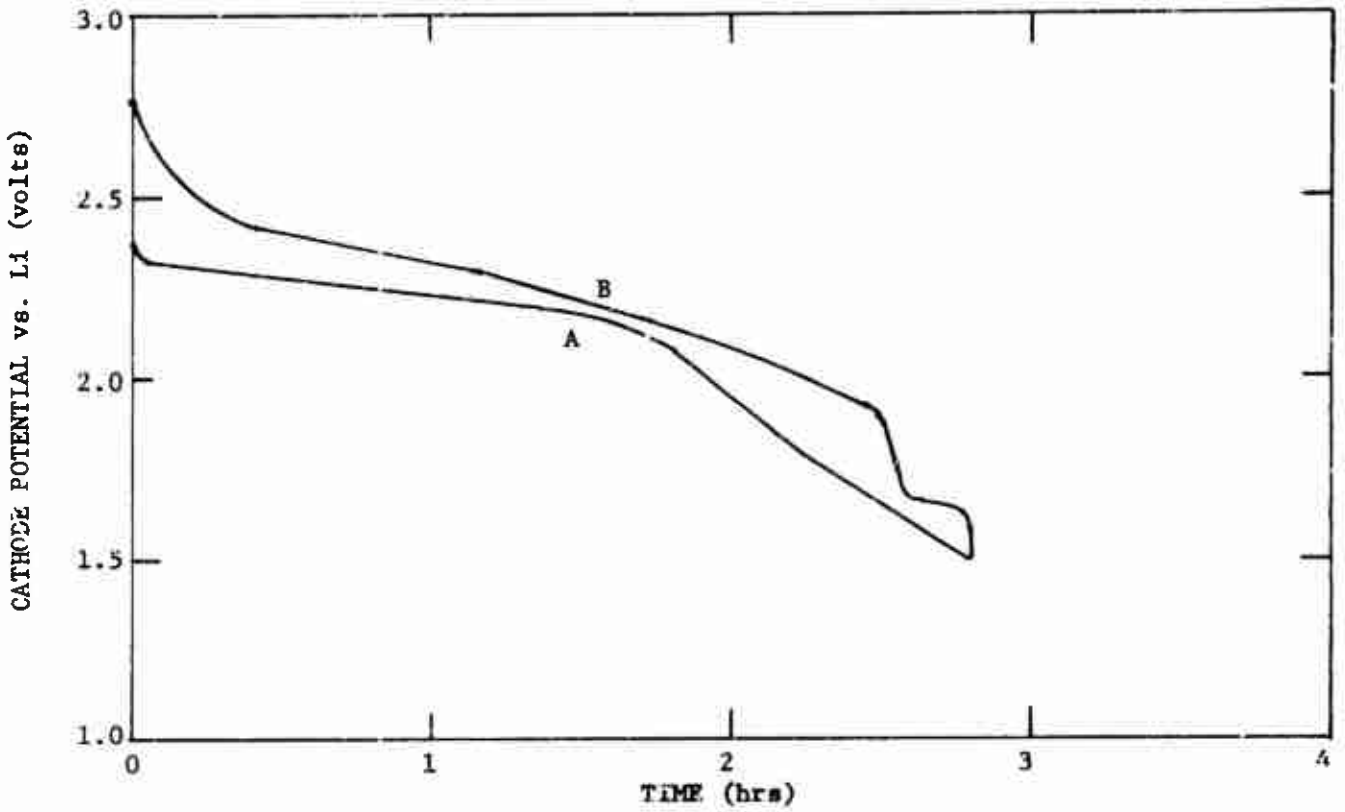


Fig. 3: One hundred and tenth discharge (A)-charge (B) cycle of $TiS_2$. PC, 1M $LiClO_4$, i = 0.78 $mA/cm^2$.

Table 2

Capacity of $TiS_2$ Foil in Refurbished Cell Cycled Galvanostatically Between +1.5V and +2.8V vs. Li

| $TiS_2$ Cycle No. | Cell Cycle No. | Capacity (equiv/mol $TiS_2$) Discharge | Charge |
|---|---|---|---|
| 145 | 1 | $0.23_0$ | $0.28_6$ |
| 149 | 5 | $0.33_9$ | $0.34_2$ |
| 154 | 10 | $0.35_2$ | $0.36_0$ |
| 159 | 15 | $0.36_5$ | $0.36_3$ |
| 164 | 20 | $0.37_5$ | $0.37_5$ |
| 169 | 25 | $0.38_0$ | $0.37_7$ |
| 174 | 30 | $0.38_6$ | $0.38_6$ |
| 179 | 35 | $0.39_4$ | $0.38_8$ |
| 184 | 40 | $0.39_4$ | $0.39_0$ |

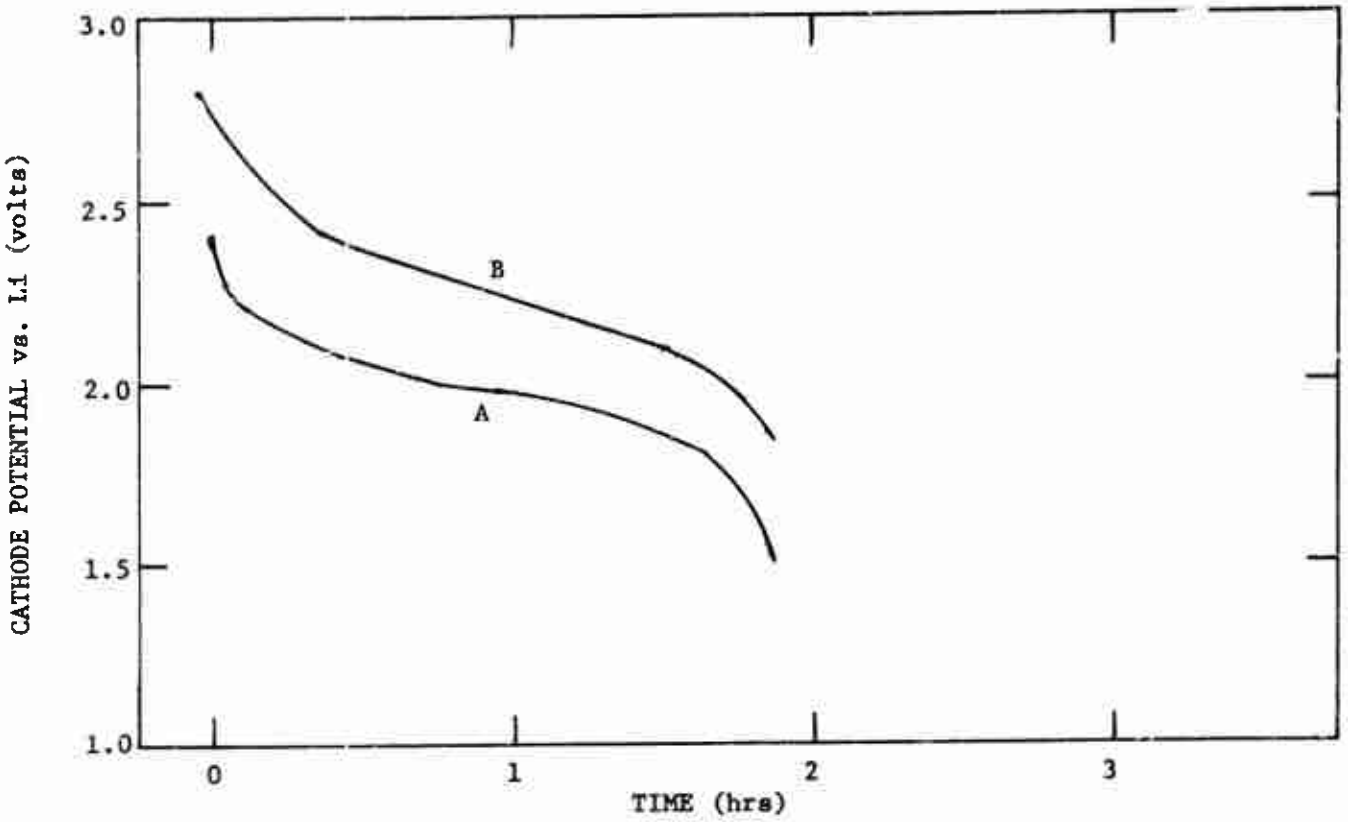


Fig. 4: Fifth discharge (A)-recharge (B) cycle of reassembled $TiS_2$ cell (149th cycle of $TiS_2$ electrode). PC, 1M $LiClO_4$, $i = 0.78$ mA/cm$^2$.

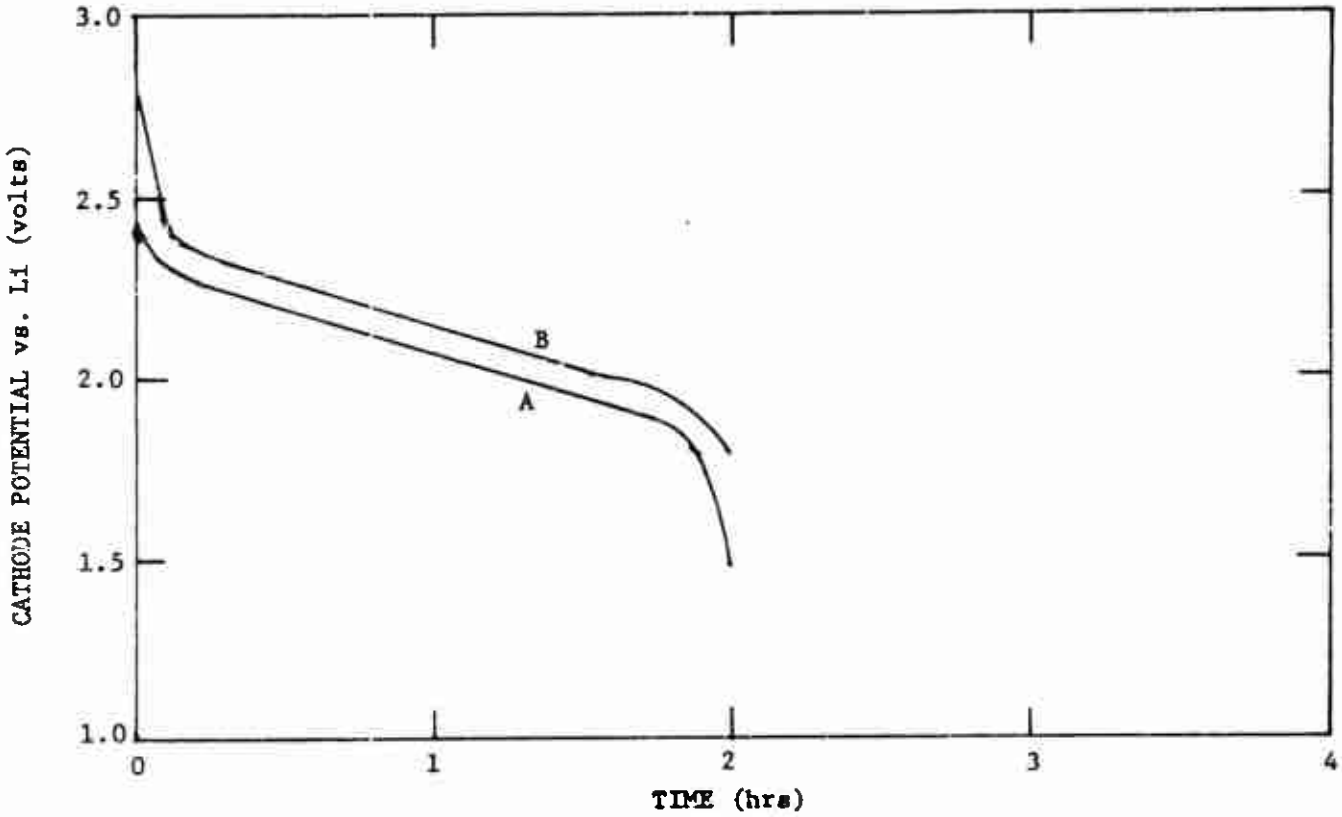


Fig. 5: Twenty-fifth discharge (A)-recharge (B) cycle of reassembled $TiS_2$ cell (169th cycle of $TiS_2$ electrode). PC, 1M $LiClO_4$, i = 0.78 $mA/cm^2$.

(b) Titanium Trisulfide

Experimental: The electrode was prepared in a two-step procedure described previously (3). The Ti metal flag was reacted with sulfur vapor first at 750°C to form the disulfide which was then converted to the trisulfide at 550°C. The cell was assembled as described above for the $TiS_2$ foil electrode. The active electrode area was 6.38 $cm^2$ with $9.34 \times 10^{-4}$ mol $TiS_3$. The cell was cycled between +1.75V and +2.8V vs. a Li reference at 5.2 mA. The potential vs. time curves were recorded. The 1M $LiClO_4$/PC electrolyte was preelectrolyzed between a carbon cloth working electrode and a lithium counter electrode using a lithium reference. The background current of this treated electrolyte was tested in an assembly identical to the test cell using a Teflon-bonded carbon black working electrode. At a carbon potential of +1.500V vs. the Li reference, the residual current was 0.26 mA.

Results: The OCP of the $TiS_3$ was 2.95V. The cycling behavior shows the same general characteristics as observed previously. The first discharge capacity is 1.4 equivalents per mol $TiS_3$, about twice that of the second cycle. During the next dozen cycles the capacity continues to decrease slightly and then reaches a constant value at 0.68 equiv/mol $TiS_3$. To date the cell reached 65 cycles. Table 3 lists the capacities of the first ten cycles and then every fifth cycle up to the 65th.

The potential reversibility improved with cycling. Figures 6 and 7 are the potential-time curves for the 11th and the 50th cycles respectively. On the 11th cycle the MDP was +2.16V and the MRD was +2.28V, while on the 50th cycle the MDP remained unchanged at +2.16V while the MRP had decreased to +2.20V. Overall, the potential reversibility was good.

In summary, the results show that titanium trisulfides can also be cycled extensively with excellent capacity retention. After the characteristic high capacity initial discharge, the electrode settled at a constant capacity of 0.68 equiv/mol $TiS_3$ which it retained over the following 60 full charge-discharge cycles at the relatively high C/3 rate. Two facts may account for the better cycling performance of this $TiS_3$ electrode compared to earlier measurements: the two-step preparation and/or the higher cutoff voltage upon discharge.

2. Effect of Cutoff Potential and Solvent

(a) Titanium Disulfide

Deep discharge cycles of titanium disulfide were investigated in PC and methyl acetate (MA). Figure 8 shows the first cycle discharge in PC. The electrode area was 6.40 $cm^2$ with $1.00 \times 10^{-3}$ mol $TiS_2$. The current density was 0.81 $mA/cm^2$. The discharge curve shows two distinct plateaus. The first at +2.15V which gradually decays to +1.80V, and the second much shorter one at +1.15V. The transition between plateaus is

Table 3

Capacity of a $TiS_3$ Foil Cycled Galvanostatically Between +1.75V and +2.8V vs. Li

| Capacity (equiv/mol $TiS_3$) | | | Capacity (equiv/mol $TiS_3$) | | |
|---|---|---|---|---|---|
| Cycle No. | Discharge | Charge | Cycle No. | Discharge | Charge |
| 1 | 1.39 | $0.76_8$ | 15 | $0.67_5$ | $0.67_3$ |
| 2 | $0.76_2$ | $0.74_3$ | 20 | $0.67_5$ | $0.67_1$ |
| 3 | $0.75_4$ | $0.73_1$ | 25 | $0.66_8$ | $0.66_8$ |
| 4 | $0.73_3$ | $0.77_3$ | 30 | $0.67_5$ | $0.66_8$ |
| 5 | $0.72_7$ | $0.71_9$ | 35 | $0.67_4$ | $0.67_5$ |
| 6 | $0.71_4$ | $0.71_4$ | 40 | $0.67_5$ | $0.67_3$ |
| 7 | $0.70_8$ | $0.70_0$ | 45 | $0.68_3$ | $0.67_7$ |
| 8 | $0.70_4$ | $0.69_8$ | 50 | $0.68_3$ | $0.67_5$ |
| 9 | $0.69_8$ | $0.70_0$ | 55 | $0.68_1$ | $0.67_5$ |
| 10 | $0.69_0$ | $0.68_3$ | 60 | $0.67_7$ | $0.67_3$ |
| | | | 65 | $0.67_3$ | $0.66_2$ |

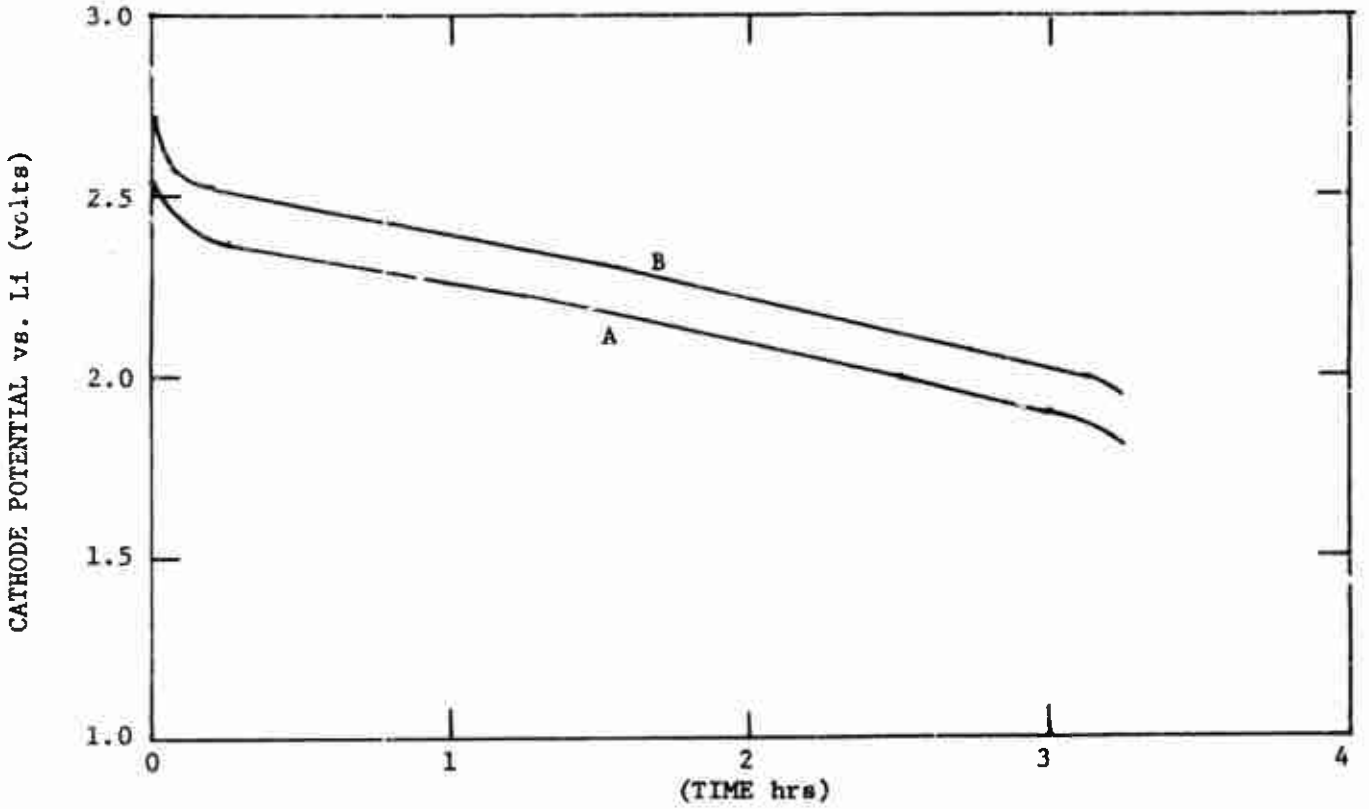


Fig. 6: Eleventh discharge (A)-recharge (B) cycle for $TiS_3$, PC, 1M $LiClO_4$, i = 0.81 mA/cm$^2$.

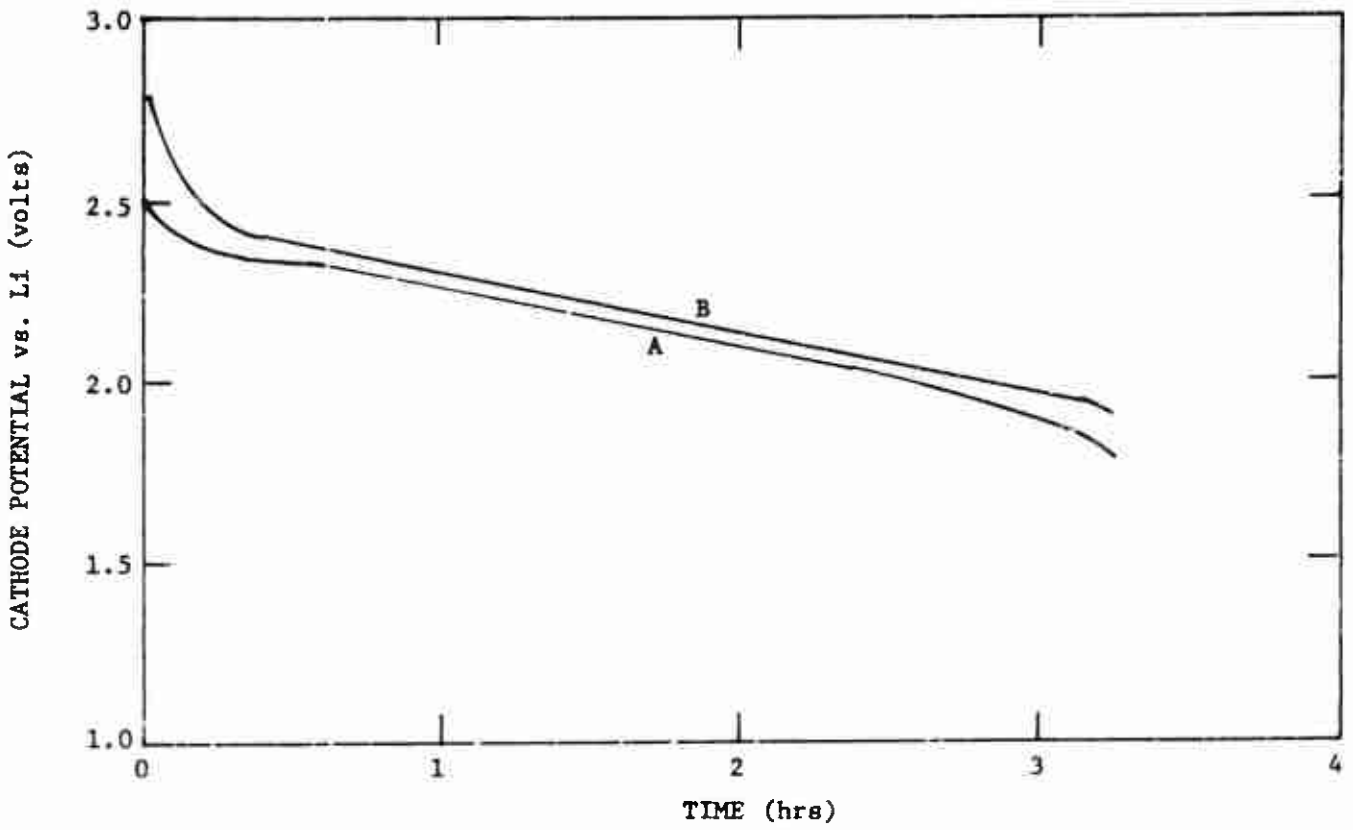


Fig. 7: Fiftieth discharge (A)-recharge (B) cycle for $TiS_3$. PC, 1M $LiClO_4$, i = 0.81 $mA/cm^2$.

sharp. The recharge potential shows a single gently sloping curve between +1.95V and +2.55V. The potential curve of the second discharge shows the same structure as the first except that the first plateau is shorter. The recharge potential curve for the second and all subsequent recharges is the same as the first except that they are shorter. On the third cycle, the second plateau on the discharge curve disappears and is replaced by an almost constant slope decay to the +0.5V lower limit. All subsequent discharges show the same behavior.

Table 4 presents the capacity data for this cell. This table lists the capacity to the lower +0.5V limit and also to the +1.5V point. The capacity associated with the lower potential discharge appears not rechargeable and decreases upon cycling. However, the capacity to 1.5V also continues to decrease slowly possibly due to irreversible changes in the $TiS_2$ or to reduction products of the electrolyte which may take place at the lower potentials.

Figure 9 shows a similar discharge of $TiS_2$ in methyl acetate. The foil electrode had an area of 6.43 $cm^2$, 1.25 x $10^{-3}$ mol $TiS_2$ and was cycled at 0.81 $mA/cm^2$. The potential behavior, while similar to the cycling in PC, shows some distinct differences. The initial voltage plateau starts at +2.25V and comes to about +1.65V before the sharp drop. However, here there is no second plateau at ∿+1.1V; the sharp transition ends at ∿+0.7V, and then the potential decays gradually to the lower limit. The recharge potential curve is similar to that observed in PC except that the potential shift on the transition from the discharge to charge condition is much sharper and the slope of the curve is less. The potential reversibility in the MA on the first cycle is improved over that in PC. The MDP of the main plateaus in PC and MA are the same at +2.15V, while the corresponding MRP are +2.15V. The potential curves for the subsequent cycles are similar to the first except that the transition from the main plateau becomes sharper.

Table 5 lists the capacity data for this cell. The cell capacity decreases with cycling as observed in the PC indicating again the loss of capacity due either to active material or electrolyte decomposition. In MA, however, the reversibility is improved. In cycles 2 through 7 the recharge capacity exceeds that obtained at +1.5V and approaches the total discharge capacity obtained at the +0.5V lower limit. The total cell capacity in MA is also greater than observed in PC.

These differences along with those observed in the potential curves indicate the solvent plays a role in modifying the behavior of the electrodes.

(b) Titanium Trisulfide

Several titanium trisulfide electrodes were subjected to deep discharge cycles in PC and MA. The results are summarized in Figs. 10,

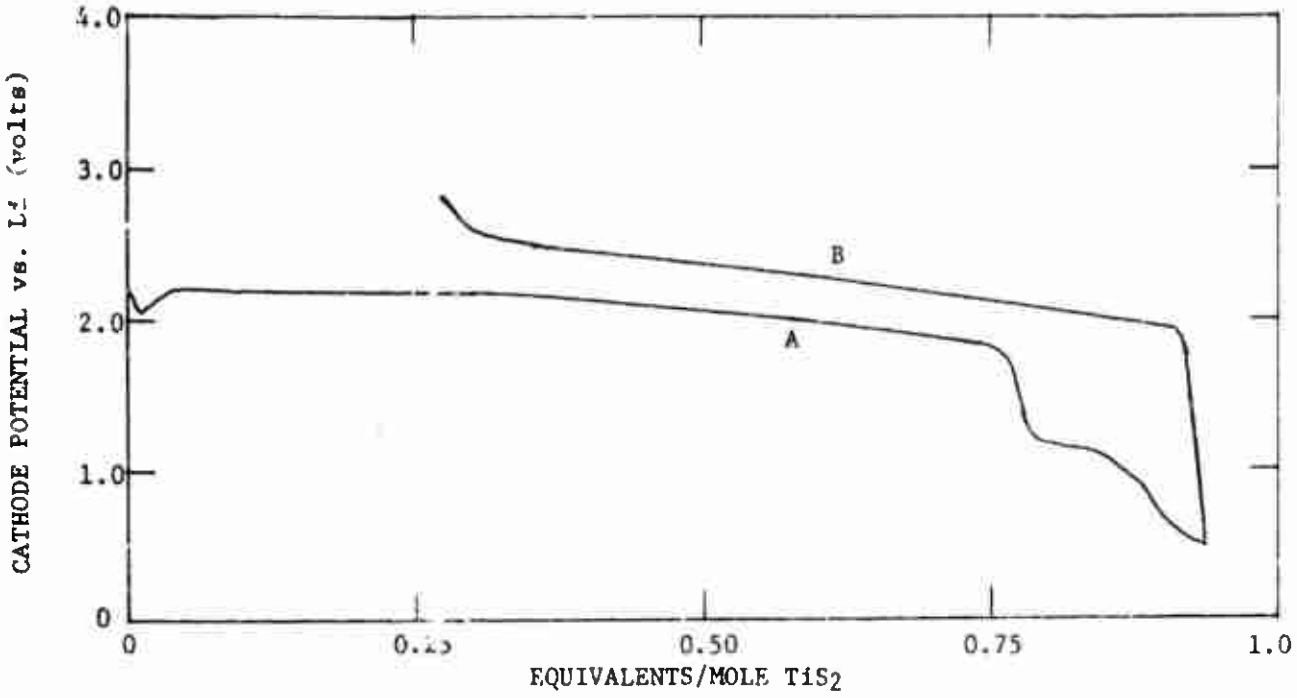


Fig. 8: First discharge (A)-charge (B) cycle of $TiS_2$, PC, 1M $LiClO_4$, $i$ = 0.81 mA/cm$^2$.

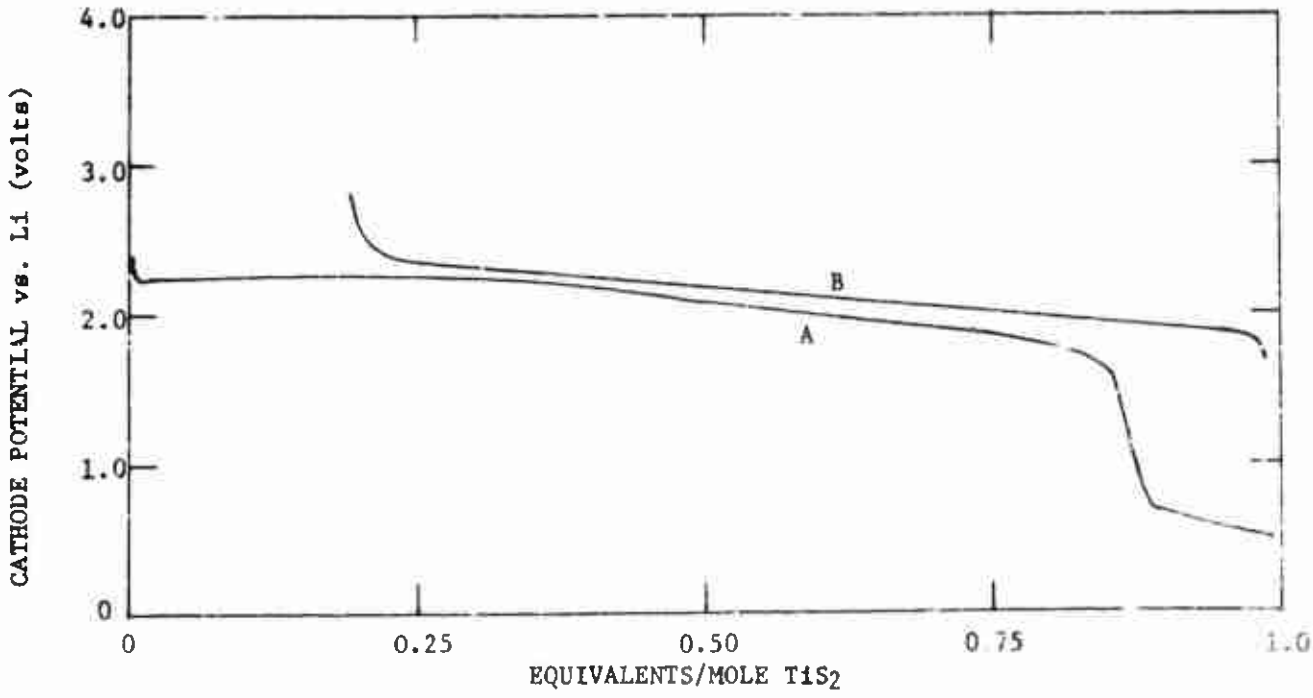


Fig. 9: First discharge (A)-charge (B) cycle of $TiS_2$, MA, 1M $LiClO_4$, $i$ = 0.81 mA/cm$^2$.

Table 4

Capacity of $TiS_2$ Foil Cycled Galvanostatically Between +0.5V and +2.8V in 1M $LiClO_4$/PC

| | Capacity (equiv/mol $TiS_2$) | | |
|---|---|---|---|
| Cycle No. | Discharge to 0.5V | Discharge to 1.5V | Charge to 2.8V |
| 1 | 0.94 | 0.67 | 0.58 |
| 2 | 0.70 | 0.57 | 0.49 |
| 3 | 0.57 | 0.52 | 0.45 |
| 4 | 0.52 | 0.50 | 0.43 |
| 5 | 0.51 | 0.50 | 0.43 |
| 10 | 0.47 | 0.46 | 0.39 |
| 15 | 0.46 | 0.45 | 0.39 |
| 17 | 0.45 | 0.44 | 0.38 |

Table 5

Capacity of $TiS_2$ Foil Cycled Galvanostatically Between +0.5V and +2.8V in 1M $LiClO_4$/MA

| | Capacity (equiv/mol $TiS_2$) | | |
|---|---|---|---|
| Cycle No. | Diacharge to 0.5V | Discharge to 1.5V | Charge to 2.8V |
| 1 | 0.99 | 0.86 | 0.80 |
| 2 | 0.93 | 0.76 | 0.80 |
| 3 | 0.79 | 0.73 | 0.76 |
| 4 | 0.77 | 0.72 | 0.74 |
| 5 | 0.74 | 0.70 | 0.74 |
| 6 | 0.72 | 0.69 | 0.71 |
| 7 | 0.70 | 0.66 | 0.66 |
| 8 | 0.65 | 0.59 | 0.51 |

11, and 12 and in Tables 6 and 7. A long sloping discharge in several mostly not very well defined potential steps is characteristic for $TiS_3$ electrodes in PC (Fig. 10). Capacities reach typically 3 and in some cases more than 3 equivalents per mol of $TiS_3$. It appears that reduction of solvent and/or impurities may also contribute to the capacity at lower potentials. For example, Fig. 11 compares the first discharge of two identical $TiS_3$ preparations (prepared simultaneously in the same ampoule) in standard electrolyte and in preelectrolyzed electrolyte. The discharges appear identical except for a reduction plateau at approximately 1.5V which is nearly absent in the preelectrolyzed electrolyte. The standard electrolyte is prepared from freshly distilled PC and dried three times with 5A molecular sieve after $LiClO_4$ dissolution. The preelectrolysis was carried out between a carbon and a lithium electrode with the carbon electrode at 1.2V vs. Li. A similar reduction plateau at ~1.3V appears to be present in the discharge of Fig. 10(a) while it is absent in the otherwise equal discharge shown in Fig. 10(b). Here, however, we cannot attribute it to a known difference in the two electrolytes. An interaction of the reduced $TiS_3$ with the solvent, a reduction product or an impurity appears likely, indicated by an onion-like odor noticed upon cell disassembly. The odor of onion is generally associated with 1-propanethiol ($CH_3$-$CH_2$-$CH_2$-SH) (2).

A deep discharge of $TiS_3$ in methyl acetate is shown in Fig. 12. The discharge curve is similar to that obtained in PC, however, the potential steps are much more marked. There are four clear plateau potentials. The long plateau at 0.6V is probably associated with solvent reduction.

The large first discharge capacity is only partially rechargeable The sloping recharge voltage too shows several potential steps suggesting that rechargeability is not restricted to a specific discharge plateau. The reaction products generated at the more cathodic potentials appear, however, less reversible indicated by a more rapid decrease of their contribution during cycling. While the capacity of the first deep discharge, without contribution of solvent reduction, reaches approximately three equivalents per mol of $TiS_3$, the recharge capacity varies significantly. It is, however, worth noting that during the early cycles values above 1 equiv/mol $TiS_3$ are obtained. During extended cycling stable capacities were sometimes close but obviously below 1 equiv/mol $TiS_3$.

In practical terms, we found that higher capacities can be obtained with $TiS_3$ by lowering the cutoff voltage on discharge. The capacity retention upon cycling appears, however, decreased by the formation of the less reversible more highly reduced reaction products of $TiS_3$ and possibly also by products reaulting from solvent or impurity reductions.

B. Potentiostatic Measurements on $TiS_2$ Electrodes

Experimental: The $TiS_2$ foil and the cell were prepared and assembled as usual. The electrode area was 6.27 $cm^2$ with $1.20 \times 10^{-3}$ mol $TiS_2$.

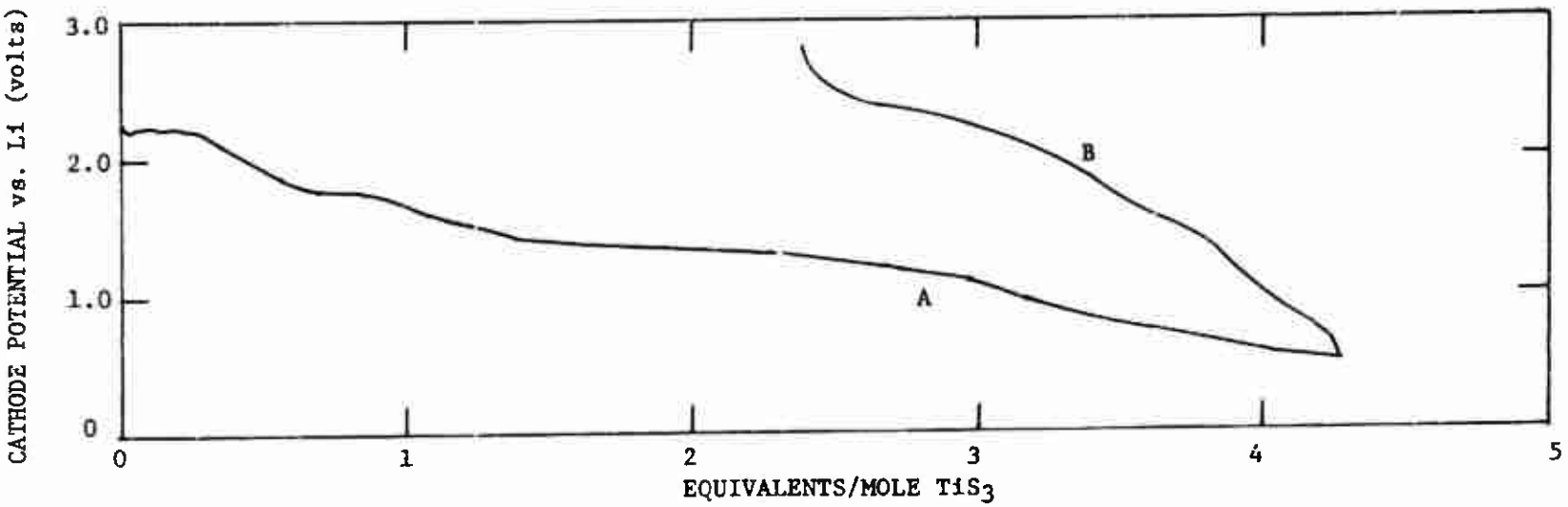


Fig. 10(a): First discharge (A) and recharge (B) for $TiS_3$ foil, 1M $LiClO_4$/PC, i = 0.84 mA/cm$^2$.

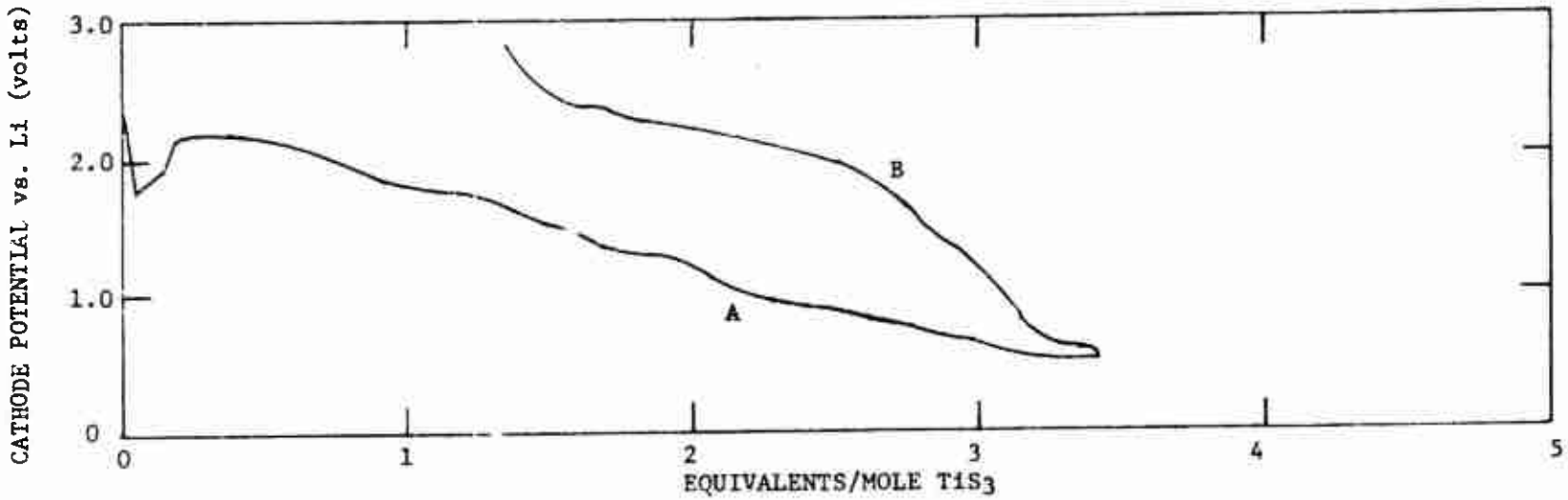


Fig. 10(b): Firat discharge (A) and recharge (B) for 750/550 $TiS_3$, 1M $LiClO_4$/PC, i = 0.84 mA/cm$^2$.

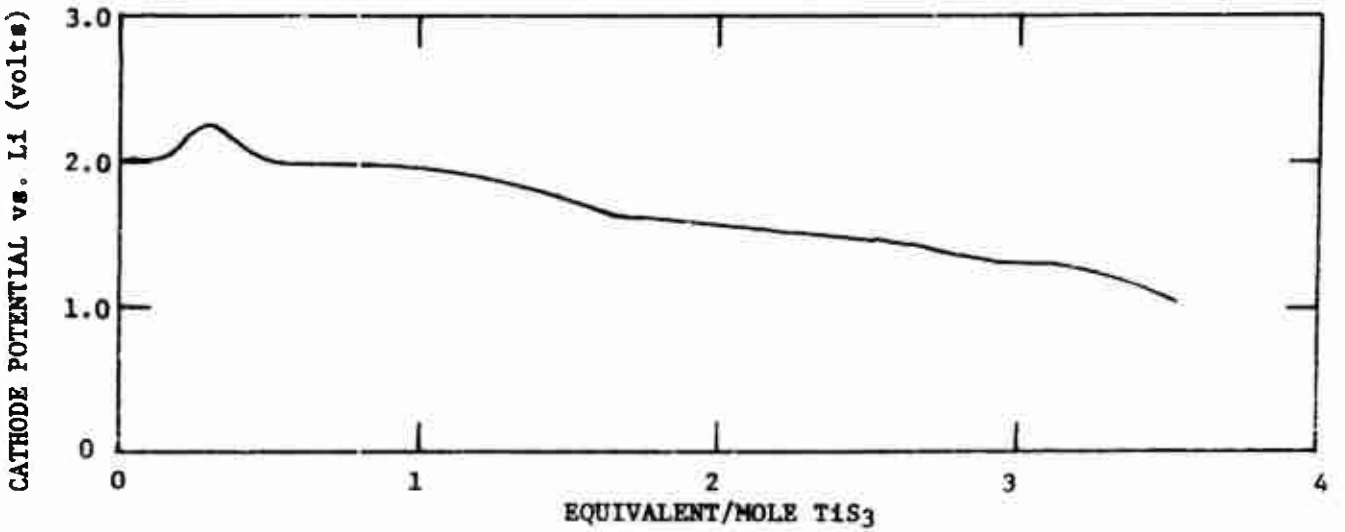


Fig. 11(a): First discharge for $TiS_3$, 1M $LiClO_4$/PC electrolyte with no pretratement. $i = 0.87\ \mu A/cm^2$.

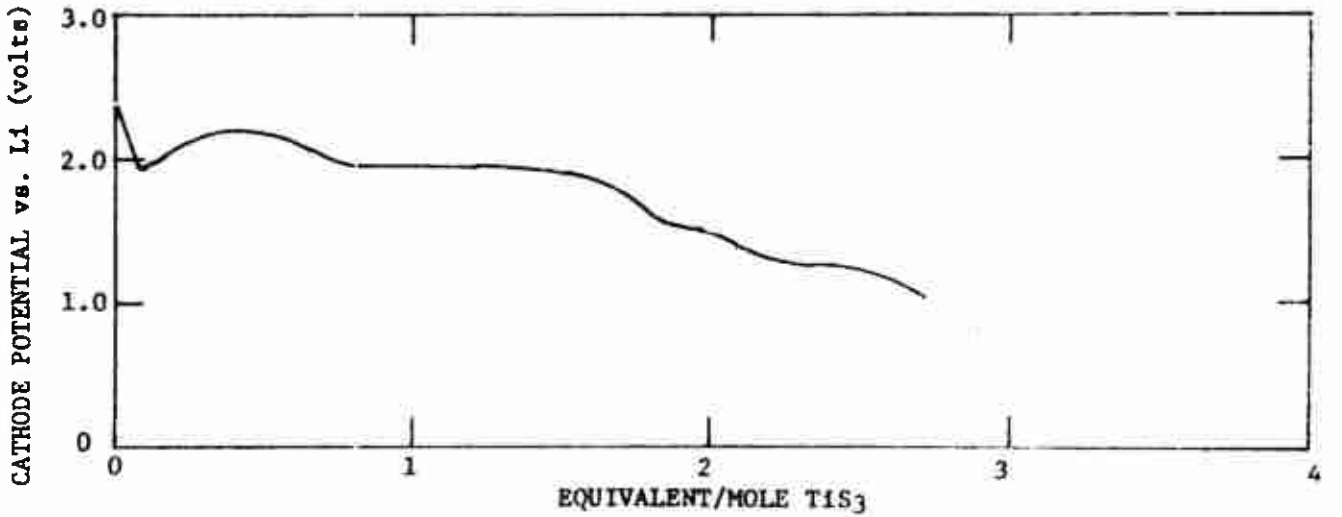


Fig. 11(b): First discharge for $TiS_3$, 1M $LiClO_4$/PC preelectrolyzed. $i = 0.84\ mA/cm^2$.

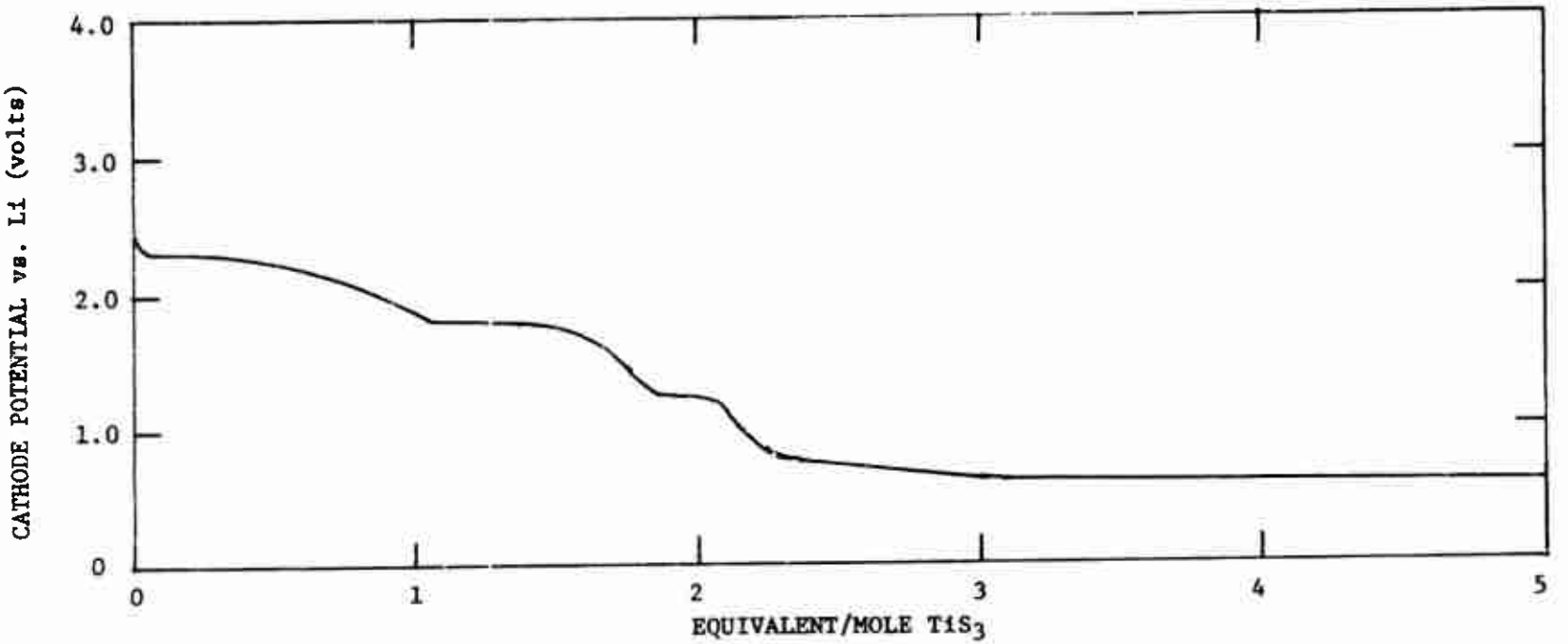


Fig. 12: First discharge for $TiS_3$, 1M $LiClO_4$/MA, i = 0.81 mA/$cm^2$.

Table 6

Capacity of $TiS_3$ Foil Cycled Galvanostatically in 1M $LiClO_4$/PC Between +0.5V and +2.8V

| | Capacity (equiv/mol $TiS_3$) | | | |
|---|---|---|---|---|
| | 550°C Preparation | | 750°C/550°C Preparation | |
| Cycle No. | Discharge | Charge | Discharge | Charge |
| 1 | 4.26 | 1.89 | 3.37 | 2.01 |
| 2 | 2.37 | 1.77 | 2.30 | 1.90 |
| 3 | 1.85 | 1.62 | 2.00 | 1.62 |
| 4 | 1.67 | 1.51 | 1.71 | - |
| 5 | 1.54 | 1.43 | - | - |
| 6 | 1.46 | 1.37 | - | - |
| 7 | 1.39 | 1.30 | - | - |
| 8 | 1.32 | - | - | - |

Capacity of $TiS_3$ Foil Cycled Between +1.0V and +2.8V at 5.2 mA with Untreated PC

| | Capacity (equiv/mol $TiS_3$) | | | |
|---|---|---|---|---|
| | Untreated Electrolyte | | Preelectrolyzed Electrolyte | |
| Cycle No. | Discharge | Charge | Discharge | Charge |
| 1 | 3.56 | 0.68 | 2.72 | 0.58 |
| 2 | 0.81 | 0.59 | 0.62 | 0.46 |
| 3 | - | - | 0.50 | 0.43 |
| 4 | - | - | 0.46 | 0.41 |
| 5 | - | - | 0.44 | - |

Table 7

Capacity of $TiS_3$ Foil Cycled Between +0.5V and +2.8V in 1M $LiClO_4$, Methyl Acetate at 5.2 mA

| | Capacity (equiv/mol $TiS_3$) | |
|---|---|---|
| Cycle No. | Discharge | Charge |
| 1 | 6.04 | 1.46 |
| 2 | 2.72 | 1.18 |
| 3 | 2.03 | 0.82 |
| 4 | 0.88 | 0.58 |
| 5 | 0.68 | 0.53 |
| 6 | 0.57 | 0.46 |
| 7 | 0.50 | 0.43 |

A PAR 373 potentiostat was used and the current recorded as a function of time. The cell was discharged at +1.500V twice and recharged at +2.800V vs. Li once. The electrolyte was preelectrolyzed 1M $LiClO_4$/PC. The initial $TiS_2$ OCP was 3.110V and after ~40 min declined to 2.954V. The experiments were terminated when the residual currents reached approximately 20 μA which required ~20 hrs.

Results: Figure 13 shows the current vs. time curves for the cell. The data presented is for the first 100 min. This time span is probably the most significant because most of the capacity is obtained within this period (e.g., first discharge 94%, first recharge 93%, and second discharge 90%). The two diacharge curves are similar except for two regions. Between 5 min and 10 min the curves are coincident, and from 45 min on they are reasonably coincident. They are significantly different between 0 and 5 min where the first discharge currents are much higher; and between 10 min and 45 min where the first discharge current actually plateaued at 27 mA, while the second discharge current showed a continual decline. The recharge current behavior was distinctly different from the discharge current. Initially it decayed much more slowly so that over the first 15 min it remained greater than either the first or second discharge current. Over the next 15 min it decayed more quickly, and from the 30 min mark on it was less than the discharge currents. Figure 14 shows the capacity in equivalents per mol $TiS_2$ vs. current. These curves were obtained by incremental integration of the current-time curves. Either a linear or exponential approximation was used. The current coordinate of Fig. 9 is the final current at the end of an integration interval. These data indicate the capacity of the $TiS_2$ to approach 0.8 to 1 mol $TiS_2$. The recharge capacities at high currents reflect the above observations that the recharge currents are initially higher for a larger period of time; thus, almost 50% of the end capacity is attained at currents above 5 mA/cm$^2$, while for the two discharge curves only 23% (first discharge) and 17% (second discharge) of the capacity was obtained at a current density above 5 mA/cm$^2$.

The capacity observed for this potentiostated electrode compares well with that of the galvanostatically cycled $TiS_2$ foil discussed above. At a current density of 0.78 mA/cm$^2$, utilizations of 0.82 vs. 0.76 equiv/mol for the first discharge, 0.78 vs. 0.61 equiv/mol for the first recharge, and 0.76 vs. 0.63 equiv/mol for the second discharge were observed for the potentiostatically and galvanostatically discharged electrodes respectively. From the potentiostatic data, a first estimate of the capacity vs. rate can be made. Figure 14 shows that the critical current density for discharge is between 1.6 mA/cm$^2$ and 4.8 mA/cm$^2$ for the $TiS_2$ foils as they are prepared here. At current densities greater than 4.8 mA/cm$^2$, ~20% of the final capacity is obtained for both the first and second discharges, while at current densities less than 1.6 mA/cm$^2$, at least 80% of the final capacity is obtained. The second discharge rate capability for the electrochemically reversible reaction does not appear significantly different from the rate of the first discharge. The apparent difference between the two (Fig. 14)

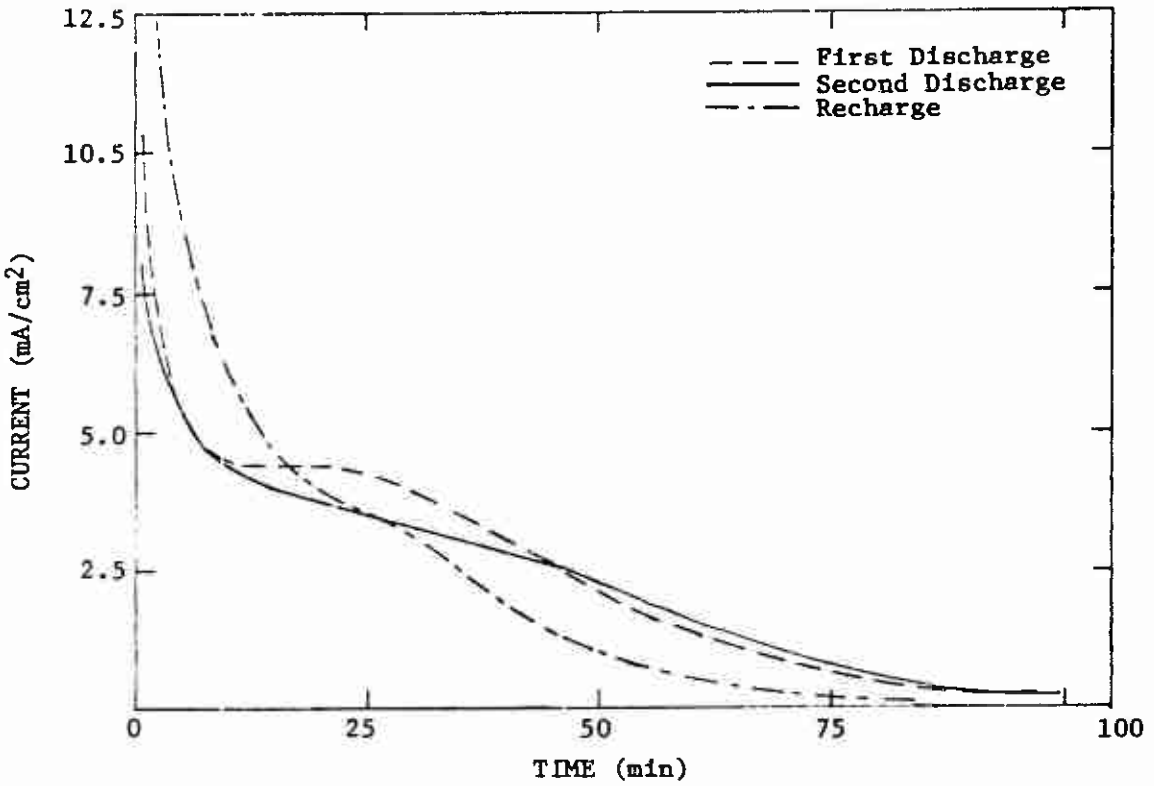


Fig. 13: Current for $TiS_2$ cycled potentiostatically, 1M $LiClO_4$/PC.

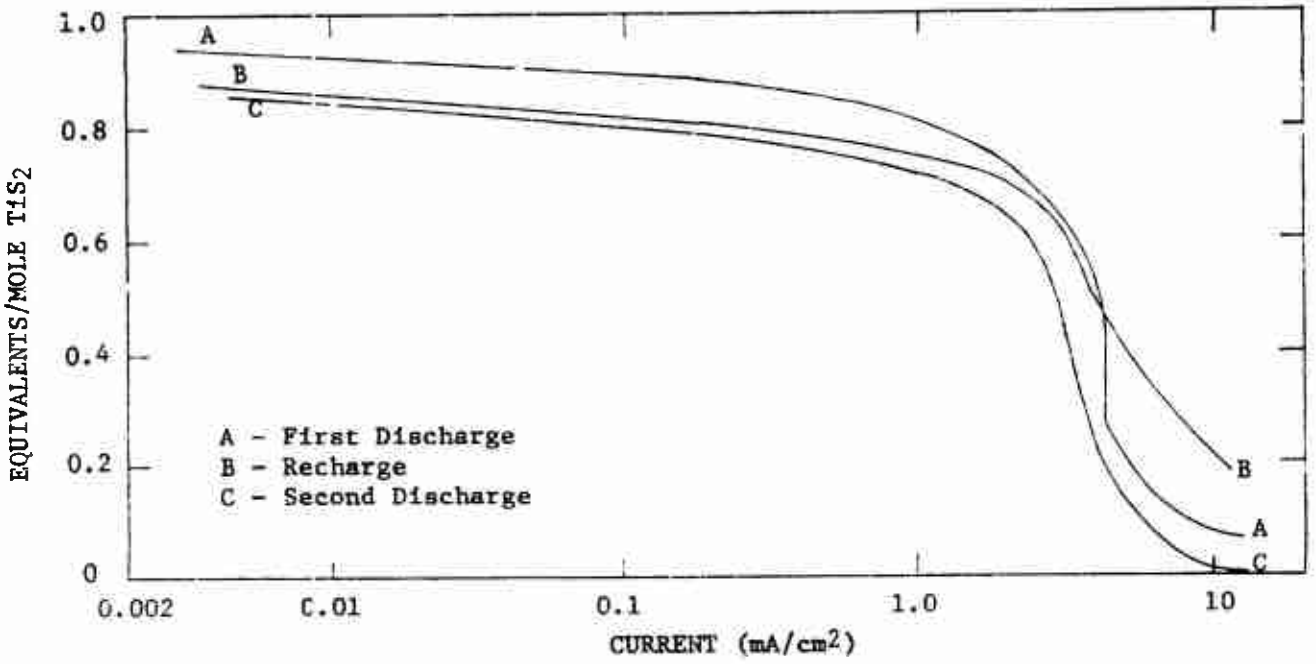


Fig. 14: Capacity of $TiS_2$ cycled potentiostatically. 1M $LiClO_4$/PC.

is probably due to the contribution to the first discharge by an irreversible reduction. This is reflected in the galvanostatic cycling as the longer first discharge. The recharge capacity is about 0.06 equiv/mol less than the first discharge. A point by point adjustment of the first discharge curve by this amount brings it almost coincident with the second discharge curve (Fig. 14) except between 15 mA and 25 mA. It also appears that the irreversibility occurs during the initial high current (>80 mA) phase of the first discharge, because at 80 mA the first discharge curve is already 0.06 equiv/mol greater than the second discharge curve.

C. Titanium-Vanadium Alloy Sulfide Electrodes

Experimental: Teflon-bonded electrodes were fabricated from a powder synthesized by the reaction of a titanium-vanadium alloy with sulfur. The alloy powder (-100 mesh), 90 Wt% Ti and 10 Wt% V, was purchased from Ventron. The sulfide was prepared by reaction of an intimate mixture of alloy and sulfur powders (molar ratio 3 mols S/1 mol alloy) in an evacuated quartz tube at 550°C for 88 hrs. There was only a slight trace of unreacted sulfur after this heating time. The product was a black, shiny powder similar in appearance to $TiS_3$ prepared by this same method. The x-ray diffraction pattern of this material showed the pattern of $TiS_3$.

Teflon-bonded electrodes were prepared as previously described on Ni Exmet screen with a mixture 80 Wt% alloy sulfide, 10 Wt% carbon black, and 10 Wt% Teflon. Two electrodes were tested. The simulated battery configuration was used with 1M $LiClO_4$/PC electrolyte. One electrode (two-sided area of 10.40 $cm^2$) was cycled between +1.0V and +3.0V at 5.2 mA (j = 0.50 $mA/cm^2$) for 22 complete cycles. The other electrode (two-sided area of 9.85 $cm^2$) was cycled between +1.0V and +3.0V at 5.2 mA (j = 0.53 $mA/cm^2$) for 20 complete cycles.

Results: The potential time curves (Fig. 15) are characterized by a two plateau discharge with mid-discharge potentials of 1.7V and 1.2V respectively. Charging also occurs in two steps. During later cycles the distinction between the two potential plateaus becomes less apparent. The potential reversibility (potential difference between discharge and recharge curves) is less favorable than in comparable electrodes of pure $TiS_3$. Variations in the structure of the bonded powder electrodes should have only a negligible effect at the relatively low rates of these cycle tests.

The changes in electrode capacity during cycling are summarized in Table 8. Overall capacity and the rate of decrease upon cycling is similar to that observed with $TiS_3$ electrodes under comparable cycling conditions.

In summary, it appears that the reduction and oxidation of $Ti_{1-x}V_xS_3$ electrode is more difficult (more cathodic and more anodic potentials)

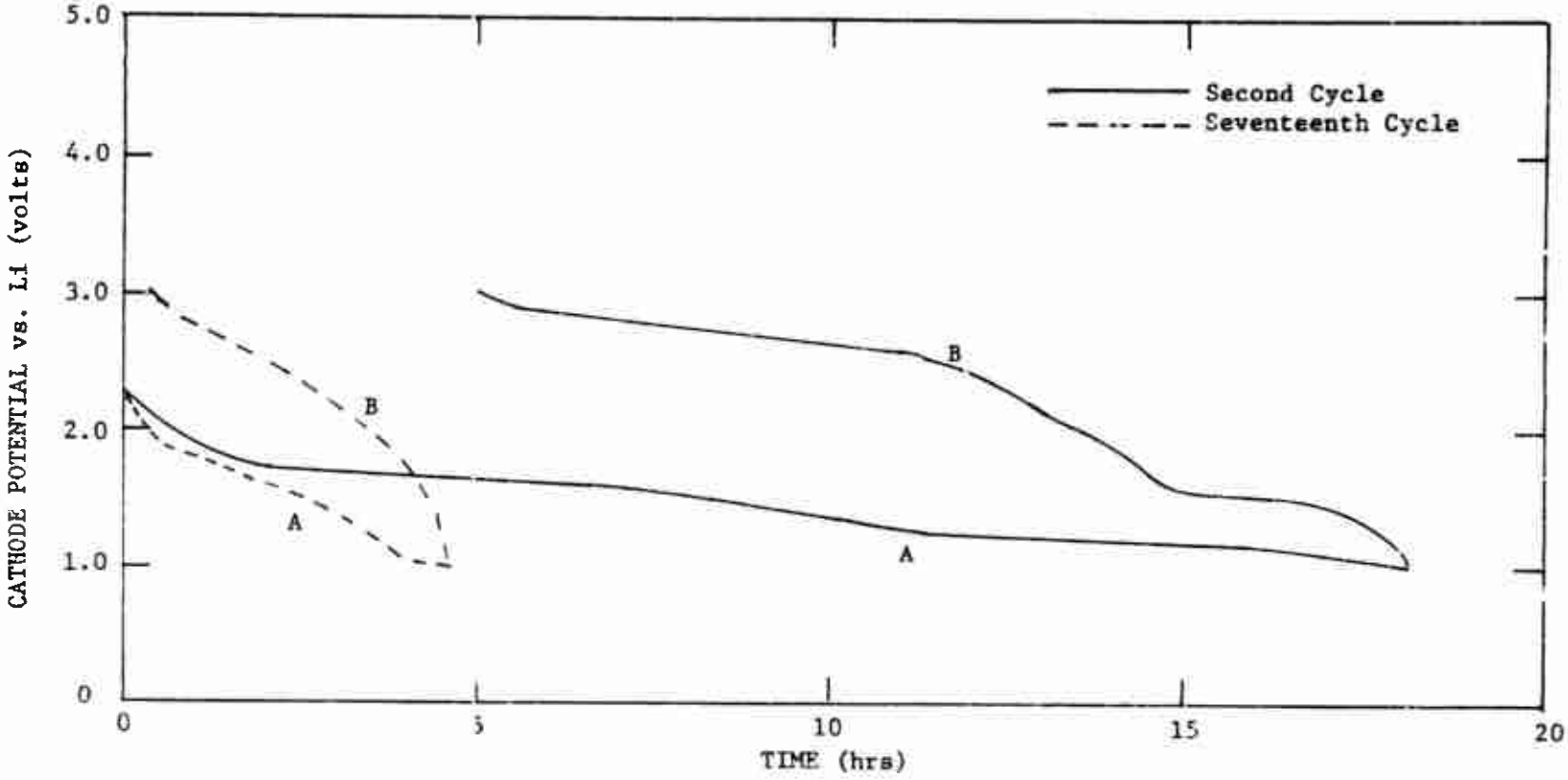


Fig. 15: Second and seventeenth discharge (A) and recharge (B, cycles for $TiVS_3$ bonded electrode. 1M $LiClO_4$/PC, $i$ = 0.50 mA/$cm^2$.

Table 8

Capacity of Two Ti, V Alloy Trisulfide Electrodes Cycled Galvanoatatically between +1.0V and +3.0V in 1M $LiClO_4$/PC

| | Capacity (equiv/mol metal atom) | | | |
|---|---|---|---|---|
| | Electrode 31-110 | | Electrode 31-121 | |
| Cycle No. | Discharge | Charge | Discharge | Charge |
| 1 | 0.63 | 0.36 | 2.13 | 1.22 |
| 2 | 2.37 | 1.67 | 2.09 | 1.44 |
| 3 | 1.99 | 1.49 | 1.42 | 1.15 |
| 4 | 1.52 | 1.31 | 1.14 | 0.97 |
| 5 | 1.31 | 1.19 | 1.10 | 0.88 |
| 6 | 1.19 | 1.11 | 0.89 | 0.82 |
| 7 | 1.12 | 1.08 | 0.81 | 0.80 |
| 8 | 1.07 | 1.02 | 0.80 | 0.75 |
| 9 | 1.03 | 0.97 | 0.71 | 0.66 |
| 10 | 0.98 | 0.93 | 0.66 | 0.64 |
| 11 | 0.92 | 0.89 | 0.62 | 0.59 |
| 12 | 0.88 | 0.84 | 0.54 | 0.52 |
| 13 | 0.82 | 0.79 | 0.47 | 0.43 |
| 14 | 0.76 | 0.74 | 0.37 | 0.34 |
| 15 | 0.74 | 0.73 | 0.31 | 0.28 |
| 16 | 0.66 | 0.60 | 0.25 | 0.23 |
| 17 | 0.59 | 0.56 | 0.22 | 0.20 |
| 18 | 0.54 | 0.51 | 0.19 | 0.18 |
| 19 | 0.49 | 0.46 | 0.17 | 0.16 |
| 20 | 0.46 | 0.43 | 0.15 | 0.14 |
| 21 | 0.42 | 0.40 | - | - |
| 22 | 0.39 | 0.35 | - | - |

than those of $TiS_3$, while overall capacity and cycle behavior show little difference under comparable cycling conditions.

## D. Discussion

$TiS_2$ and $TiS_3$ electrodes can tolerate extensive electrochemical discharge-charge cycling. The $TiS_2$ system appears more clearly defined due to its apparent simplicity. It is characterized by a single discharge and charge plateau with excellent potential reversibility. The reduction product is an intercalation compound of $TiS_2$ and Li. Limiting capacities measured both galvanostatically and potentiostatically approach a value of one equivalent per mole of $TiS_2$. This is in excellent agreement with a model in which the octahedral interstitial sites in the $TiS_2$ layer lattice are occupied by $Li^+$ ions. Reversible capacities obtained with actual electrodes during extended cycling (in excess of 100 cycles) are approximately 0.6 equiv/mol $TiS_2$. Initial discharge capacities are, in general, between 0.75 and 0.95 equiv/mol $TiS_2$. Values below one should be expected even in the limiting case for most of our samples since they represent titanium rich disulfides where the excess metal atoms randomly occupy the octahedral interstitial sites in the metal sulfide layer lattice.

Galvanostatic and potentiostatic measurements showed that the rate capability of the $TiS_2$ electrodes is quite high. For example, in our electrodes 60% of the capacity can be obtained above 3 $mA/cm^2$ and over 80% above 1 $mA/cm^2$. It is worth noting that the recharge can be carried out at even higher rate. For example, over 70% of the capacity can be recharged above 3 $mA/cm^2$ with our electrodes. Diffusion of $Li^+$ ions in the solid originally appeared to be the rate limiting steps. The pronounced plateau in the potentiostatic current-time curves (Fig. 13) suggests, however, more complex reaction kinetics. The experimental behavior can be explained by a mixed diffusion control in the electrolyte solution, and in the metal sulfide. The initial high current depletes the viscous PC electrolyte of $Li^+$ ions close to the $TiS_2$ and results in a limiting current corresponding to the plateau value. Later, when the rate of $Li^+$ absorption into the sulfide decreases due to the longer diffusion distance in the solid, this process becomes rate determining.

The titanium trisulfide system is more complicated than the disulfide. The discharge occurs through several plateaus. The initial discharge capacity is significantly higher for the trisulfide ($\sim$3 e/$TiS_3$ vs. $\sim$1 e/$TiS_2$); however, since the later discharge plateaus are only partially rechargeable, the reversible capacity appears to eventually reach the same value of approximately 0.6-0.7 equiv/mol $TiS_3$. The break in the first plateau of the initial discharge which is particularly clear in methyl acetate appears to be due to the same intercalation process observed with the disulfides. The further, less reversible reaction may involve the breaking of the disulfide bond or the occupation of different positions in the crystal lattice. The better cycling performance of the trisulfides of Nb and Ti prepared by the conversion of the disulfide may be associated with a

distorted trisulfide structure resulting from the retention of some structurel elements of the disulfide. The trisulfide of a titanium (90%) vanadium (10%) alloy shows the same capacity behavior as the $TiS_3$, however, the discharge plateau has a lower potential indicating that it is more difficult to reduce this alloy sulfide.

The difference in behavior of the disulfide and the trisulfide has the following implication for their use in practical batteries. In general, the $TiS_2$ appears more attractive for a battery, since it has a very flat discharge potential above 2.0V and a higher capacity retention per equivalent weight upon extended cycling with an energy density of 130 Whr/lb based on active materials. For specialized applications involving only a limited number of discharge-charge cycles, the $TiS_3$ may be advantageous due to its higher energy density during approximately the first 10 cycles.

## III. SUMMARY AND FUTURE WORK

Our measurements have shown that both $TiS_2$ and $TiS_3$ electrodes can be cycled extensively (in excess of 100 cycles). Initially, $TiS_3$ electrodes show higher capacities than $TiS_2$ electrodes. After approximately 10 cycles, electrodes of both sulfides cycled with constant capacity of 0.6 equivalents per mol of sulfide. For $TiS_2$, this corresponds to an energy density of 130 Whr/lb based on the active materials. The discharge cutoff voltage, the solvent (PC or methyl acetate), and the $TiS_3$ preparation procedure appear to affect the cycling behavior.

Potentiostatic measurements on $TiS_2$ showed that charge and discharge reactions are relatively rapid. Typical electrodes can deliver 60% of their capacity at current densities above 3 $mA/cm^2$. The recharge reaction is even more rapid. Diffusion of $Li^+$ ions in the sulfide lattice and in the electrolyte appear to be rate limiting.

Titanium-vanadium trisulfide electrodes show lower discharge voltages (1.7V). Capacity and cycling behavior is similar to $TiS_3$.

During the next quarter we will continue to investigate the charge and discharge reaction of niobium and titanium sulfide electrodes in PC and methyl acetate electrolytes. We will further cycle titanium trisulfide and disulfide cells in order to more closely characterize cycling behavior including the effect of current density and temperature.

## IV. REFERENCES


1. G. L. Holleck et al., Second Quarterly Report, ECOM-74-0072-2, December 1974.

2. F. Challenger and D. Greenwood, Biochem. J., 44, 87 (1949).